Crystallization of Anatase from Amorphous Titania Using the Hydrothermal Technique: Effects of Starting Material and Temperature

Kazumichi Yanagisawa * and James Ovenstone

Research Laboratory of Hydrothermal Chemistry, Kochi University, Kochi 780-8520, Japan

Received: February 11, 1999; In Final Form: May 12, 1999

The crystallization of anatase from amorphous titania has been controlled using the hydrothermal technique. Crystallite size and surface area can be controlled by careful alterations of the hydrothermal conditions. The catalytic effect of the water on crystallization has been demonstrated, and the crystallization mechanism has been shown to change from a solid-state type to dissolution precipitation as the temperature is increased. The influence of the amorphous precursor preparation route has been examined in order to evaluate the effect of contaminant ions on the crystallization process. It has been shown that the chloride ion accelerates the nucleation of the anatase, even under dry conditions. The effects of acidic and basic solutions have been studied. Acidic conditions result in the formation of anatase, brookite, and rutile, whereas basic conditions accelerate the production of anatase. The mechanisms for the hydrothermal crystallization of anatase and rutile are discussed.

Introduction

The high photocatalytic activity of titania has been well documented,[1−3] and it is also well-known that it is the anatase polymorph rather than the brookite or rutile polymorphs that has the highest photoactivity. Commercial photocatalysts, however, fail to provide a phase-pure anatase titania photocatalyst. The most active commercially available catalyst (Degussa P25) has an anatase content of 60−80%.[4] The difficulty in producing an extremely active, phase-pure anatase photocatalyst stems from the fact that rutile is the thermodynamically stable polymorph, and although anatase is kinetically stable, it is readily converted to the rutile phase in the temperature range 600−1000 °C. It is therefore desirable to find a low-temperature route for the synthesis of the anatase phase, to avoid conversion to rutile. Furthermore, control of the physical properties of the anatase itself is important in determining its photocatalytic activity.

It is widely regarded that an anatase powder with a high surface area, but also a high degree of crystallinity, with a large crystallite size is desirable to enhance the photocatalytic activity, since such a powder will have relatively few disruptions in its electronic band structure. These properties are, of course, difficult to achieve at the same time, and so a powder whose crystallites have fewer flaws would be ideal. Many approaches have been used to obtain well-crystallized titania. The sol−gel method has a number of disadvantages, in that the precursors are relatively expensive, the temperature required to form anatase is high, and the anatase produced is acidic and unstable.[5−7] The coprecipitation method also has the problem of a high crystallization temperature.[8] On the other hand, hydrothermal processing has shown great promise, producing highly active photocatalysts at relatively low temperatures (around 300 °C). However, even these powders required calcination at the higher temperature of 550 °C to reach their full photocatalytic potential.[9−11]

The current work aims not only to produce phase-pure anatase, but also to determine the mechanism by which it, and rutile, are formed under hydrothermal conditions. The final goal is predictive control over the quality of the anatase product powders. Therefore amorphous titania powders have been prepared by a number of routes and treated in a variety of types of hydrothermal solution at different temperatures, to determine the effects of contaminant ions, acid, base, temperature, and time upon the crystallization process, and determine a likely mechanism for the crystallization of anatase.

Experimental Section

Amorphous titania was prepared from three different routes.

(1) $TiCl_4$ (30 mL, 0.273 mol) was diluted with ice cold water (300 mL). A 1.5 M NH_3 solution was added dropwise to the clear $TiCl_4$ solution until the pH was raised from 0.5 to 3.0 (approx. 740 mL). The white precipitate formed was aged for 24 h before washing with water until the pH reached 7. The amorphous powder (A3) was then dried for 24 h at room temperature.

(2) $TiCl_4$ (20 mL, 0.182 mol) was diluted with ice-cold water (200 mL), and added dropwise to a 7.5 M ammonia solution. The pH fell from 12.5 to 10.9 as the white precipitate formed. Again the amorphous precipitate was aged for 24 h before washing until the pH reached 9.2. The amorphous powder (B3) was then dried for 24 h at room temperature.

(3) $Ti(OC_2H_5)_4$ (25 g) was added to 550 mL of dry ethanol and mixed thoroughly before being added to a 0.6 M solution of water in ethanol [5.94 mL (0.33 mol) water in 550 mL ethanol]. After aging for 25 min, the reaction mixture was centrifuged and washed twice with ethanol before drying in a vacuum desiccator.[12]

The simplest crystallization treatment was carried out by dispersing 30 mg of amorphous titania powder in 10 mL (50 % fill) of distilled water in a Hastelloy-lined autoclave, and then heating the autoclave to a variety of temperatures and for varying lengths of time. Salt solutions were sometimes used in place of water. For "dried salt" reactions, the amorphous powder was suspended in a 1 M salt solution for 1 week, before washing and drying. The powder was then treated dry in an autoclave at

* Author to whom correspondence should be addressed.

10.1021/jp990521c CCC: $18.00
Published on Web 08/31/1999

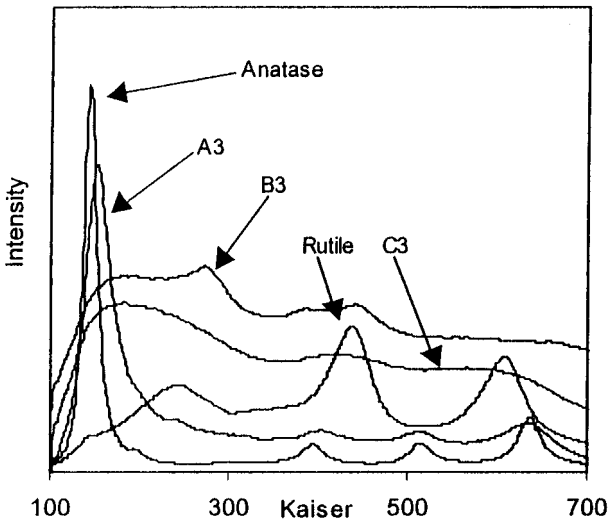

Figure 1. Raman spectra of titania starting materials.

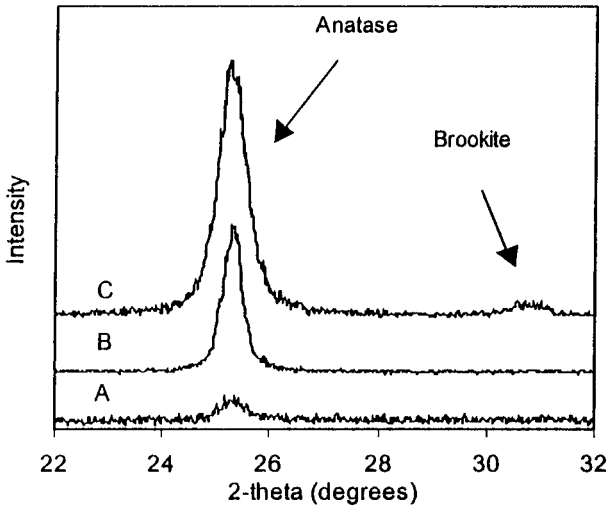

Figure 2. XRD traces of the C3 titania powders after dry treatment (A), treatment in vapor (B), and hydrothermal treatment (C) at 250 °C for 1 h.

250 °C. Dry treatment involved drying the powder under vacuum at room temperature for 24 h prior to treatment in a dry autoclave at 250 °C. Treatment in vapor was carried out by keeping the amorphous powder in a controlled humidity environment for 24 h at 30 °C before treatment in an autoclave at 250 °C. The A3 powder contained 34.7 wt % water resulting in a homogeneous pressure of 0.3 MPa at 250 °C, the B3 powder contained 30.6 wt % water (0.28 MPa), and the C3 powder contained 32.1 wt % water (0.29 MPa).

After treatment in the autoclaves, the powders were washed with water and dried at room temperature under vacuum. The phase was determined by XRD (Rigaku Rotaflex), and the crystallite size was estimated by Scherrer's method. The specific surface area was measured using the 3 point BET method using a Yuasa Ionics NOVA 1000 instrument. TG/DTA was carried out on a Seiko SSC5200H system. The TG/DTA apparatus was used to calcine samples by heating at a ramp of 20 °C min^{-1} to 1000 °C before allowing to cool. The phase of these samples was then checked again by XRD, and the anatase/rutile composition estimated by the method outlined by Spurr and Myers.[13] Raman spectroscopy was carried out using a Kaiser Optical Systems Holoprobe VPT System.

Results and Discussion

XRD of the amorphous titania starting materials showed no peaks present. This technique is, however, only sensitive to the long-range order in a material, and so Raman spectroscopy was used to study the short-range order in the "amorphous" starting materials. The results clearly showed the presence of the anatase phase short-range order in the A3 powder but not in the B3 or C3 powders (Figure 1). This implies that the anatase nuclei were already present in the starting powder for A3, but that B3 and C3 were truly amorphous. The specific surface areas (measured by BET) for all three starting materials were high at over 350 m^2 g^{-1}. The A3 powder must also contain some Cl^- ion contamination, since it was washed only with water. The B3 powder is considered to have some NH_3 contamination.

Effect of Water. Figure 2 shows the XRD spectra for the products after treatment of the C3 powder for 1 h at 250 °C in dry, vapor, and hydrothermal conditions, and demonstrates the strong influence that water has upon the crystallization of anatase. In all cases where water was present, anatase was produced, with no rutile present. The powder treated in a dry atmosphere exhibited considerably less crystallinity than the powders treated in either vapor or hydrothermal conditions, and after short reaction times remained amorphous. Therefore the presence of even a little water in the reaction atmosphere catalyzes the crystallization step. This is in agreement with results previously published for anatase crystallized from amorphous titania precipitated from titanium tetraethoxide.[14]

Specific surface area data and crystallite size data (Figure 3) complement each other well, and show that the crystallization of the powder under dry conditions resulted in little growth or surface area reduction with time after the initial anatase formation in under 30 min. This was also true of the powders treated in vapor conditions. The hydrothermal product had a smaller crystallite size and specific surface area, than either the dry-produced or vapor-produced powders, which both still retained some high surface area amorphous material. This demonstrates that it is the nucleation step rather than the growth step which is accelerated most by the presence of water since the lower surface area shows that more of the high surface area precursor has been used up, while the low crystallite size implies that little growth has occurred.

The presence of water in the crystallization reaction catalyzes the rearrangement of the TiO_6 octahedra in the amorphous titania by adsorption to the titania surface, increasing the rate of crystallization dramatically. Fine crystals are produced as the nucleation rate increases, but the epitaxial crystal growth mechanism is soon hindered by the water since the rapid nucleation leaves little material for further growth. After all the amorphous starting material is used up, crystallite growth eventually takes place by the dissolution precipitation mechanism, which is slow at this temperature compared to the initial rapid growth region. TEM, was used in an attempt to examine the crystallite microstructure, but the crystallites proved to be too small to obtain clear images.

Effect of Contaminant Ions. Figure 4a shows the XRD traces for powder C3, which was treated as a dry powder at 120 °C for 90 min, after soaking in salt solution for one week, before washing and drying at room temperature under vacuum. Most of the products were amorphous, but for both the chloride salt reactions, there is a small peak corresponding to the 100% intensity peak of the anatase phase. This, combined with the absence of peaks for all the other salts, implies that the chloride ion is enhancing the crystallization of the anatase phase under dry conditions. Figure 4b shows the XRD patterns for C3, after

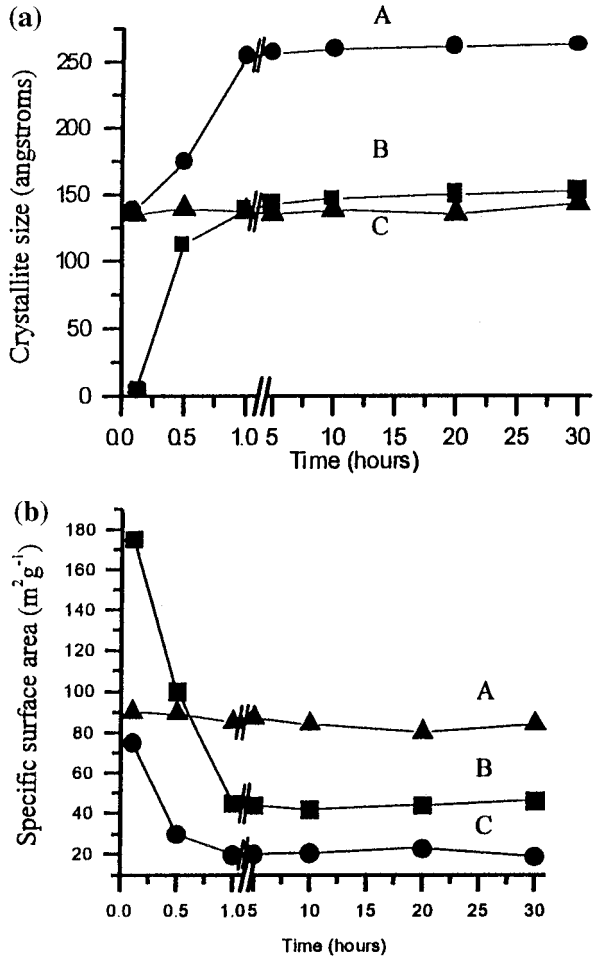

Figure 3. (a) Crystallite size vs time for C3 powders after dry treatment, treatment in vapor, and hydrothermal treatment at 250 °C. (A) Vapor-treated powder, (B) dry-treated powder, (C) hydrothermally treated powder. (b) Specific surface area vs time for C3 powders after dry treatment, treatment in vapor, and hydrothermal treatment at 250 °C. (A) Dry-treated powder, (B) vapor-treated powder, (C) hydrothermally treated powder.

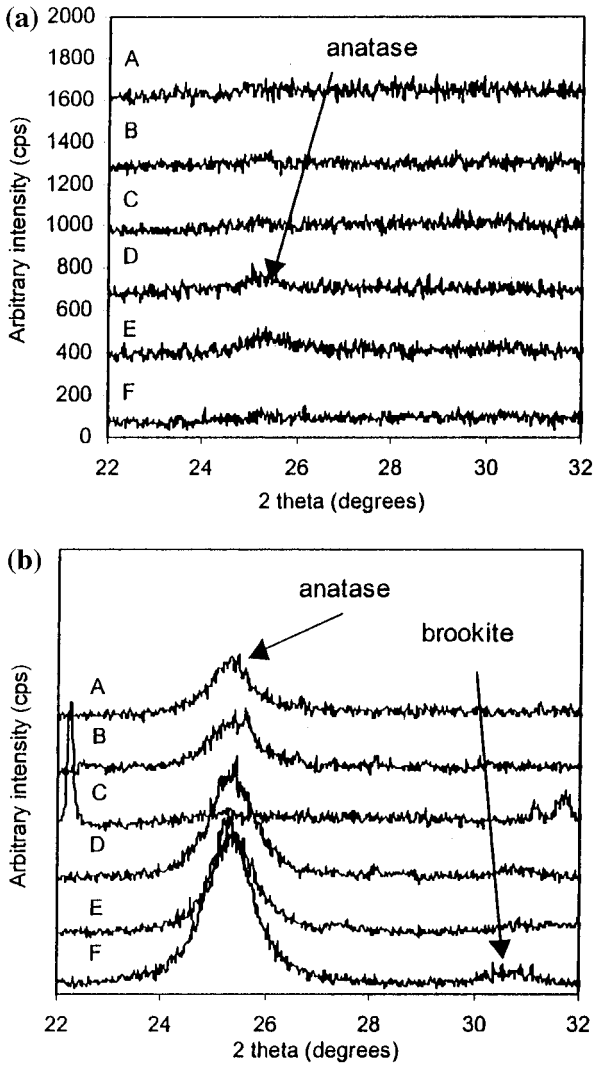

Figure 4. (a) XRD spectra of powder C3 after soaking in 1 M salt solution for 1 week, followed by dry treatment at 120 °C for 90 min. (A) K_2SO_4, (B) Na_2SO_4, (C) NaF, (D) KCl, (E) NaCl, (F) H_2O. (b) XRD traces for the C3 powders after hydrothermal treatment in 1 M salt solutions. (A) K_2SO_4, (B) Na_2SO_4, (C) NaF, (D) KCl, (E) NaCl, (F) H_2O.

hydrothermal treatment at 120 °C for 90 min in the presence of 1 M solutions of the same salts. The reaction using only water produced what appeared to be the most crystalline product, closely followed by the chloride salts. The sulfates were next, and finally sodium fluoride, which did not produce anatase at all, but a different compound. This will be discussed elsewhere. Crystallite size data showed that although the chloride solutions produced what appeared to be less crystalline products, the particle sizes where actually slightly higher, and surface areas lower. The progressively lower amounts of crystallization for the chloride, sulfate, and fluoride salts could be attributed to the increasing charge-to-size ratio, which results in stronger adsorption to the titania surface, reducing the surface/solution ion exchange, and hindering structural reorganization.

The chloride ions present in the A3 powder must be bound to the surface of the powder. These chemisorbed species will cause a certain amount of disorder in the lattice due to the differing charge and size between the oxygen and chloride ions, as has been shown in the NaCl dry reaction with C3. It has already been shown elsewhere that the crystallization of anatase proceeds initially by a solid-state rearrangement rather than dissolution precipitation,[14] and so, as the chloride ions will cause this lattice disruption, even in the absence of water, the nucleation is aided. The B3 powders on the other hand have no chloride contamination, and the surface-bound species are hydroxyl ions which cause no lattice disruption at all.

Effect of the Contaminant Ions in the Original Amorphous Powders. Experiments under dry, vapor, and hydrothermal conditions, similar to those used for the C3 powder, were carried out for the A3 and B3 powders. It is immediately clear from Figure 5 that the influence of water was far greater on the B3 powder than the A3 powder, since the A3 powder showed some crystallization even under dry conditions after 1 h, whereas the B3 powder did not. In addition, all crystallite sizes were higher for B3 powders than for A3 powders (Figure 6). Also, even under the relatively slow crystallization conditions of a dry atmosphere, no crystallite growth was observed with increasing time for the A3 powder after the initial growth in the first hour. Vapor treatment also resulted in almost no crystallite growth for A3, when compared to the B3 powder, which experienced a large amount of crystallite growth under the vapor conditions. Therefore, it is clear that the A3 powder is influenced less by the hydrothermal treatment because it is already nucleated before treatment, and that it is the chloride ion contamination that is responsible for this early nucleation. In addition, the chloride does not enhance the crystallite growth, but only the nucleation,

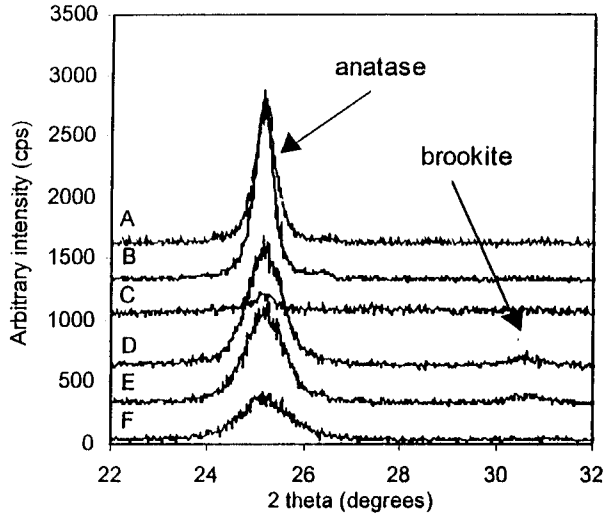

Figure 5. XRD traces of the A3 and B3 titania powders after dry treatment, treatment in vapor, and hydrothermal treatment at 250 °C for 1 h. (A) B3 hydrothermal, (B) B3 vapor, (C) B3 dry, (D) A3 hydrothermal, (E) A3 vapor, (F) A3 dry.

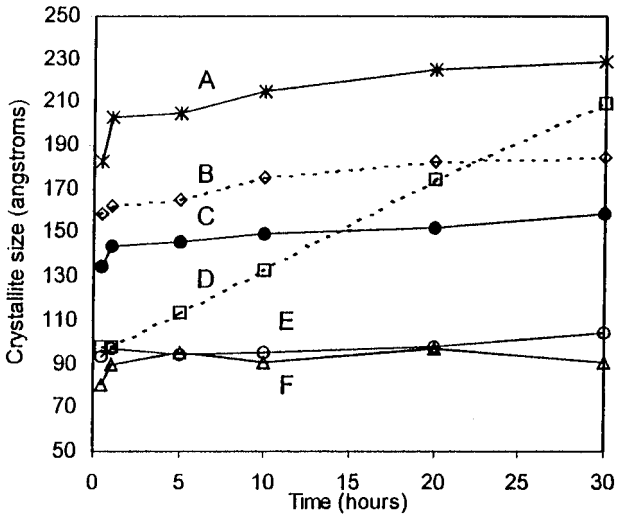

Figure 6. Crystallite size vs time for A3 and B3 powders after dry treatment, treatment in vapor, and hydrothermal treatment at 250 °C. (A) B3 vapor, (B) B3 hydrothermal, (C) B3 dry, (D) A3 hydrothermal, (E) A3 vapor, (F) A3 dry.

even under dry conditions giving very similarly shaped size vs reaction time curves.

At temperatures up to 250 °C, time does affect the crystal growth significantly; however, at 250 °C, as the dissolution/precipitation mechanism becomes more important, there is more crystallite growth with increasing time. This can be seen at 250 °C for A3 and B3 in Figure 6, but for C3, this growth is not apparent until the higher temperature of 300 °C. This can be explained in terms of the contaminant ions acting as mineralizers, improving the solubility of the powder at lower temperature, so that dissolution precipitation can occur.

Looking at the 100 °C reaction (Figure 7) where very short reactions of just 5 min were conducted, it can be seen that the surface area drops rapidly for the first 5 min for the A3 powder, but the specific surface areas of the B3 and C3 powders do not change rapidly during the first 5 min. Raman spectroscopy showed that for the A3 and C3 powders there is little change in the short-range order of the powder over the first 5 min; for the B3 powder, however, it can be seen that a significant amount of anatase-like short-range order has become apparent, despite

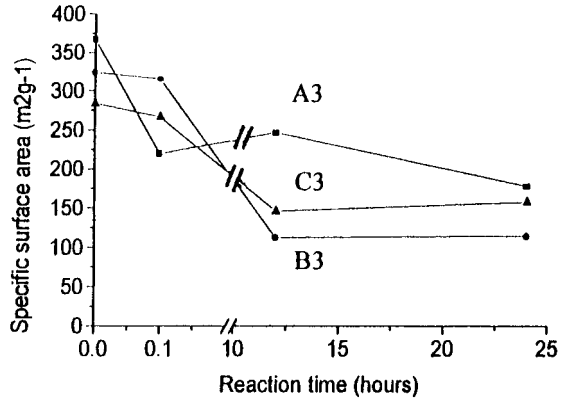

Figure 7. Specific surface area vs reaction time curves for powders treated hydrothermally at 100 °C.

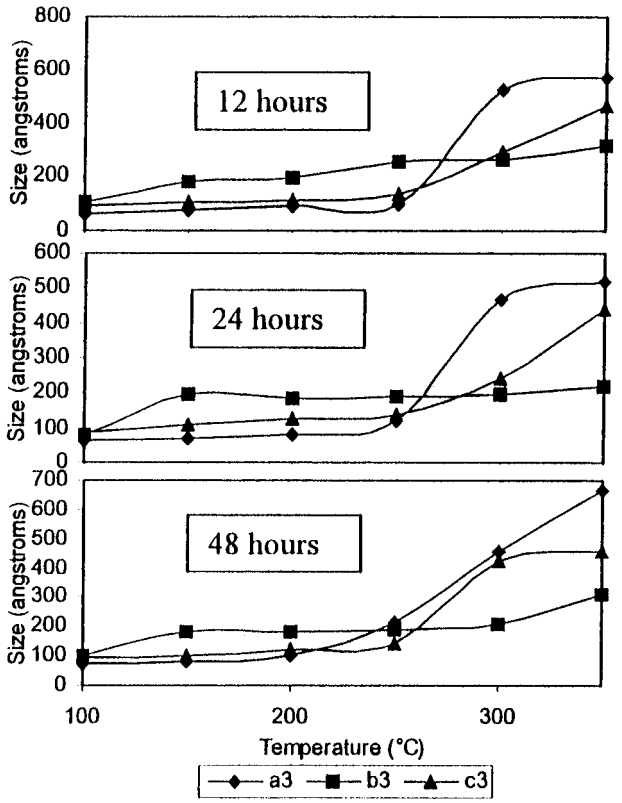

Figure 8. Crystallite size vs temperature graphs for 12, 24, and 48 h hydrothermal reactions.

the negligible change in surface area. Therefore the nucleation stage does not significantly affect the surface area, but it is the initial growth stage which causes the rapid reduction in surface. It is also evident that this process occurs faster in the B3 powder.

Effect of Temperature. Figure 8 demonstrates the effect of temperature on the anatase crystallite sizes of the hydrothermally produced powders. The points of particular interest, however, are the steps in the crystallite size curves and the different shapes of the curves for the different starting materials. For the A3 and C3 powders, the crystallite size remains constant until around 250 °C, where there is a growth region, although the size and position of the step varies from starting material to starting material, for each reaction time. The B3 powder, in contrast, produces an almost straight line of constant crystallite size after the longer initial growth region at low temperature up to 150 °C.

The change in the crystallite size at around 250 °C suggests a change in the growth mechanism from solid-state epitaxy to

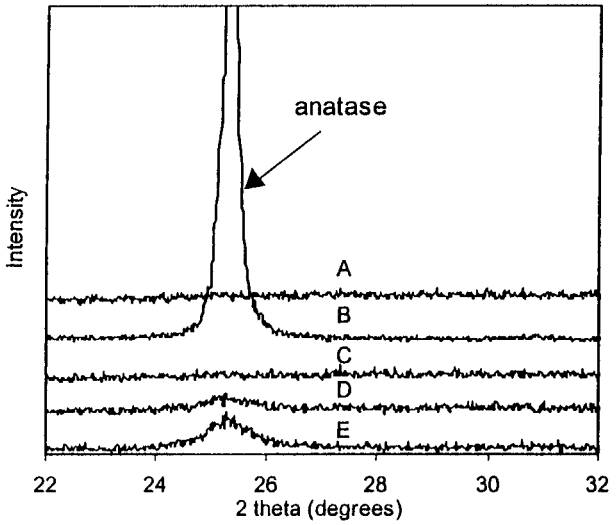

Figure 9. XRD spectra of C3 powders after hydrothermal treatment in basic solutions. (A) 0.5 M NH_3, 120 °C, 5 h; (B) 0.5 M NH_3, 250 °C, 90 min; (C) 0.5 M NH_3, 120 °C, 90 min; (D) 0.05 M NH_3, 120 °C, 90 min; (E) 0.01 M NH_3, 120 °C, 90 min.

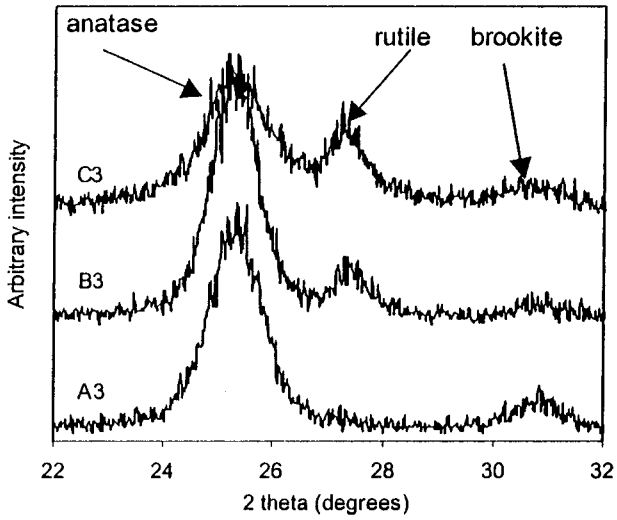

Figure 10. XRD traces of powders treated in acidic hydrothermal conditions 0.5 M HCl, 250 °C, 5 h.

dissolution/precipitation, since in this region the ionic product of the crystallization medium increases rapidly, allowing far greater solubility for the amorphous titania, as well as faster transport kinetics. The contaminants present are expected to affect the rate of growth more at lower temperatures, as they are surface species, and the surface/solution exchange increases with temperature.

This can be explained as follows. The nuclei present in the A3 powder exhibit limited growth up to 250 °C. At this temperature, the growth mechanism changes from an epitaxial growth route to a dissolution precipitation mechanism, and rapid crystallite growth is observed for the A3 powder at higher temperatures. The B3 powder, initially, is completely amorphous, and so there are no anatase nuclei available for growth until the nucleation occurs. This nucleation under hydrothermal conditions is fast for the B3 powder, as has been shown earlier, and results in the removal of almost all the amorphous material very rapidly, so that there is very little left for crystallite growth by the solid-state epitaxial mechanism after nucleation starts. The material has a higher crystallinity, and therefore lower solubility, reducing the significance of the change in mechanism to dissolution/precipitation. This can be seen by the only slight changes in the slopes of the crystallite size curves. The C3 powder has no initial nuclei, but has a slower nucleation rate than the B3 powder, due to the absence of base, which will be discussed later. The C3 powders react in a fashion similar to the B3 powders, but still have more small soluble crystallites, due to slower kinetics in the absence of base. This means that the behavior lies between the two other titania materials, since it has an intermediate crystallite size and solubility, and indeed, the size vs time/temperature graphs do show smaller steps, occurring at higher temperatures, than the A3 powder.

Effect of Acid and Base. As has been discussed earlier, in the case of the B3 powders, a mildly basic (caused by the slight contamination by residual base in the amorphous powder) hydrothermal solution can produce more crystalline anatase products with larger crystallite sizes than a neutral or slightly acidic solution at shorter reaction times (<24 h). Figure 9, however, shows the effect of using basic solutions of different concentrations, times, and temperatures upon the crystallinity of the product powder after reactions of 90 min at 120 °C. At low temperature, as the base concentration is increased, then the crystallinity of the anatase is reduced, until a completely amorphous powder is produced using a 0.5 M ammonia solution. At the higher temperature of 250 °C, however, the anatase phase has reemerged, more crystalline than any of the other reactions after 90 min. A further increase in reaction time, up to 5 h, results in a further increase in crystallite size from 27.9 to 32.5 nm. The solubility of the titania in the different types of hydrothermal solution was investigated by quenching the reactions after 90 min by dropping the autoclaves into water. ICP was then used to measure the titanium content of the supernatant fluid. The results showed that a 0.5 M ammonia solution contained 6 times that of distilled water after the 90 min hydrothermal reaction at 120 °C. The presence of the base results in a higher solubility for the titania at higher concentration, and increasing the temperature increases this solubility. This, however, is only the first stage of a two-stage process, since at higher temperature, there is even more material in solution, and the energy of the solution is sufficient to cause enough high-energy collisions between dissolved titania units to allow nucleation of anatase. Once nucleation occurs, growth by the dissolution precipitation mechanism is rapid.

The use of acidic hydrothermal conditions (0.5 M HCl solution at 250 °C for 5 h) for powders A3, B3, and C3 (Figure 10) resulted in a slight reduction in the crystallite size of the anatase produced when compared to the distilled water reactions. As the acidity increased, so the crystallite size gradually decreased. The presence of acid also resulted in the formation, in all cases, of a small amount of a second phase, which appeared to be the titania polymorph, brookite. This phase was only present in small amounts. The C3 powder also showed the presence of some rutile in the product. The product was calculated to be 47% rutile and 53% anatase. A little rutile (25.6%) was also detected in the B3 powder treated under these conditions. Rutile was not present in the A3 product.

These results point to the acid causing a change in the crystallization mechanism, lowering the activation energy for the brookite and rutile formation. The mechanism for this reaction almost certainly involves the protonation of the surface of the amorphous titania, blocking the possibility of an otherwise kinetically favorable anatase formation. ICP results showed that a 0.5 M HCl solution contained 50 times more titania than the 0.5 M solution of ammonia, and 300 times more than distilled water after the 90 min hydrothermal reaction at 120 °C. Since the chloride ion has already been shown to enhance anatase

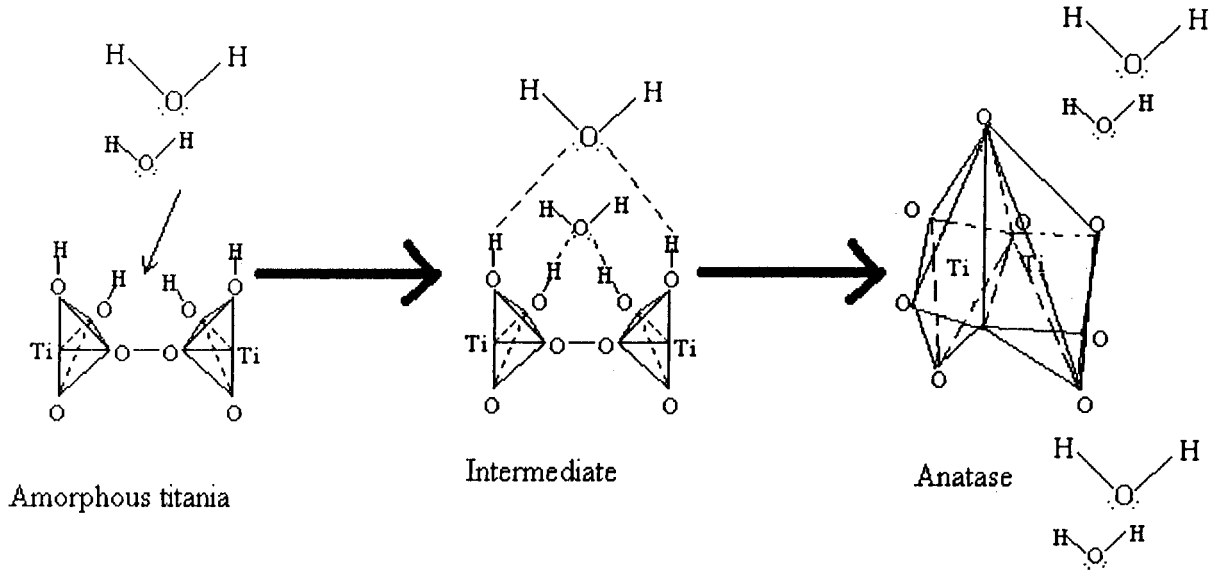

Figure 11. Reaction scheme for hydrothermal crystallization of anatase.

nucleation, it is considered to have no role in rutile formation. Increasing the time of reaction from 90 min to 5 h at 120 °C in the presence of 0.5 M acid resulted in a more crystalline solid being produced, with larger XRD peaks, for both anatase and rutile.

Mechanism of Anatase and Rutile Nucleation. From the above results, a mechanism for the crystallization of anatase and rutile has been postulated. The key to the differences in anatase and rutile formation stem from the structure of the two polymorphs. Anatase consists of TiO_6 octahedra, which share faces, while rutile TiO_6 octahedra share only edges, and the phase transformation is accomplished by the rearrangement of these octahedra.

For anatase, the rearrangement under hydrothermal conditions of these octahedra from the amorphous state proceeds by a solid-state reaction, where water molecules form bridges between surface OH groups of different octahedra which share only one common vertex, using the two lone pairs of electrons on the oxygen (Figure 11). Due to the size of the water bridges, it is possible for two bridges to form between the two octahedra, thus linking them by a triangular face. Having thus aligned the octahedra correctly, a dehydration occurs, and the original two water molecules are lost, along with two further water molecules, leaving the two titanium ions linked by two further oxygen ion vertexes, and thus sharing a face (anatase). The presence of a small quantity of base increases the rate of this reaction by increasing the concentration of OH surface groups, and thus giving an increased number of potential bridging sites. As the base concentration is increased further, however, the most active surface sites become solubilized first as the solubility of the titania increases, removing the sites for fastest anatase nucleation. The high temperature and high base concentration combination, however, results in rapid crystallization because a dissolution precipitation mechanism becomes favorable instead. The observed effect of the chloride ion in increasing the crystallization rate under dry conditions can also be attributed to bridge formation by coordination to the Cl^- ion when it is in low concentrations. In high concentrations, its effect is similar to the high base concentration, creating a negatively charged surface, repellent to itself. The larger effects observed in the A3 powder compared to the doped C3 powder, are due to the existence of anatase nuclei in the original amorphous starting material. The higher charge of the sulfate ion results in stronger bonding to the TiO_2 surface so that the activation energy for the breaking of the bridge and formation of anatase is higher, thus slowing the mobility and the reaction rate.

The use of low acid concentrations at low temperature (120 °C) in the reaction medium results in lower anatase crystallization, since the hydronium ion (H_3O^+) is unable to form bridges as there is only one available lone pair of electrons on the oxygen. As the acid concentration is increased, the surface of the titania becomes protonated, and the titania becomes solubilized. This allows a dissolution precipitation mechanism to operate, resulting in the formation of rutile. At the same time, there is still some formation of anatase due to the solid-state mechanism described above. The observed formation of just rutile at higher temperatures (>600 °C)[15] is an effect of higher solubility and faster reaction kinetics due to higher temperature, which increases the rate of the dissolution/precipitation mechanism more than the solid-state mechanism.

Conclusions

The current work has demonstrated the effectiveness of water as a catalyst for anatase crystallization. The positive effect on anatase formation of small amounts of certain contaminant ions has been shown, particularly for basic conditions, and the influence of temperature and time described and explained. A change in reaction mechanism from solid-state to dissolution-precipitation has been noted at around 250 °C. The importance of the preparation route for the amorphous precursor has been demonstrated. A model for the crystallization mechanism for anatase and rutile under hydrothermal conditions at low temperature (<250 °C) has been proposed, and the effects of the contaminant ions explained. From the results obtained, the most promising candidates for photocatalytic applications are the A3 powder treated hydrothermally at 350 °C for 48 h, giving a high crystallite size, or the B3 powder treated hydrothermally for 24 h at 250 °C, if a large surface area produces a more significant effect. The determination of which of these factors most powerfully influences the photocatalytic activity will be the focus of our research to come.

Acknowledgment. The authors thank Dr. Kanoe of the Shikoku National Industrial Research Institute for his help in

carrying out the Raman measurements. This project was funded by the EU/JSPS Joint Fellowship Program.

References and Notes

(1) Hattori, A.; Yamamoto, M.; Tada, H.; Ito, S. *Chem. Lett.* **1998**, *8*, 707.

(2) Fox, M. A.; Dulay, M. T. *Chem. Rev.* **1993**, *93*, 341.

(3) Sopyan, I.; Murasawa, S.; Hashimoto, K.; Fujishima, A. *Chem. Lett.* **1998**, *10*, 723.

(4) Dayte, A. K.; Riegel, G.; Bolton, J. R.; Huang, M.; Prairie, M. R. *J. Sol. State Chem.* **1995**, *115*, 236.

(5) Ding, X.; Liu, L.; Ma, X.; Qi, Z.; He, Y. *J. Mater. Sci. Lett.* **1994**, *13*, 462−464.

(6) Ding, X.; Qi, Z.; He, Y. *J. Mater. Sci. Lett.* **1995**, *14*, 21−22.

(7) Ichinose, H.; Kawahara, A.; Katsuki, H. *J. Ceram. Soc. Jpn.* **1996**, *104*, 914−917.

(8) Chiou, B.; Tsai, Y. J. *J. Mater. Sci. Lett.* **1989**, *8*, 485−489.

(9) Kominami, H.; Takada, Y.; Yamagiwa, H.; Kera, Y.; Inoue, M.; Inui, T. *J. Mater. Sci. Lett.* **1996**, *15*, 197−200.

(10) Kominami, H.; Matsuura, T.; Iwai, K.; Ohtani, B.; Nishimoto, S.; Kera, Y. *Chem. Lett.* **1995**, *11*, 693−694.

(11) Kominami, H.; Kato, J.; Kohno, M.; Kera, Y.; Ohtani, B. *Chem. Lett.* **1996**, *12*, 1051−1052.

(12) Barringer, E. A.; Bowen, H. K. *J. Am. Ceram. Soc.* **1981**, *65*, C199.

(13) Spurr, R. A.; Myers, H. *Anal. Chem.* **1957**, *29* (5), 760.

(14) Yanagisawa, K.; Yamamoto, Y.; Feng, Q.; Yamasaki, N. *J. Mater. Res.* **1998**, *13* (4), 825.

(15) Matthews, A. *Am. Mineral.* **1976**, *61*, 419−424.